

VOLTAGE-FREQUENCY CONTROL OF A SELF EXCITED INDUCTION GENERATOR

Eduardo Suárez and Gustavo Bortolotto

Department of Electrical Engineering

Universidad Nacional del Sur

Av. Alem 1253, (8000) Bahía Blanca, Argentina

Abstract: A new strategy for controlling voltage and frequency of a self excited induction generator (SEIG) is presented. The SEIG operates in the linear region of the core magnetizing curve, so that efficiency and performance are upgraded. An external excitation circuit, comprising permanently connected capacitors and electronically switched inductances is used. The external circuit allows to compensate for the generator reactive demand. A detailed analysis is performed, showing some salient aspects related to the connection of the external excitation circuit on the control performance. Asynchronous switching is used, but some important considerations must be taken into account related to the instantaneous phase angle between stator voltage and external inductor current at the switching instant, if good transient response is desired. Sliding mode controllers are proposed, showing good dynamic response and robust behavior upon changes in load and generator parameters. Computer simulations are used to demonstrate the validity of the proposed scheme.

Keywords: Self Excited Induction Generator, Variable Structure Control.

I. INTRODUCTION

Currently, there is a growing interest towards the utilization of renewable energy sources in the generation of electric power. In most cases, induction generators are used, driven by wind or hydraulic turbines. This is mainly due to their high reliability, low price and reduced maintenance costs.

Induction generators can operate connected to a power network or as autonomous generators. When the induction generator is connected to an infinite power net, the analysis becomes simple [1], since the voltage and frequency are determined by the driving network. However, an autonomous induction machine is able to generate electric power only if self excitation occurs [2, 3], and it can be sustained. In this latter case, the analysis is more involved;

as it will be discussed later, the operation in the linear region of the core magnetizing curve is inherently unstable, and closed loop operation is imperative. Furthermore, voltage and frequency control are interactive.

There exists a large amount of bibliography on the subject, but most applications operate the generator in the saturation region of the core. This guarantees stable operation, but the range of output voltage is limited and the efficiency is low. Using this operation mode, some authors make a transient analysis [4, 5], while others only consider stationary models to discuss the performance [6, 7, 8].

In this paper, we consider a self excited induction generator (SEIG) operating in the *linear zone* of the core magnetizing curve. The main advantages of this operation mode are: *i*) there is always margin to increase or to decrease the magnetizing flux, and consequently the generated voltage; *ii*) overall efficiency is improved. The strategies proposed here for controlling both voltage and frequency are based on variable structure control theory (VSC) with sliding mode [9, 10]. This theory has been widely applied in recent years to control electric drives [11, 12, 13, 14]. Sliding mode control offers interesting characteristics such as robustness to parametric uncertainties and external perturbations, system reduction, fast dynamic response, easy controller design for nonlinear systems, and it turns to be very appropriate for the on-off behavior of power switches.

A dynamic model of the generator is used to design the controller and to analyze the transient response of the system upon sudden load changes. A detailed analysis on the behavior of the electrical variables at the switching instants is performed. A new strategy based on variable structure control is used to regulate the frequency. Computer simulations are presented to show the transient behavior.

II. STATEMENT OF THE PROBLEM

The self excitation phenomenon, using external capacitors is well known. If operation in the linear zone of the magnetizing curve is desired, a precise (variable) leading current has to be supplied to keep with varying loads of different power factor. There are numerous possibilities to generate leading reactive power with solid state equipment. Most of them can be found under "power factor controllers" in the literature [15, 16]. Among them, the self controlled

PE-177-EC-0-2-1998 A paper recommended and approved by the IEEE Electric Machinery Committee of the IEEE Power Engineering Society for publication in the IEEE Transactions on Energy Conversion. Manuscript submitted June 18, 1997; made available for printing March 2, 1998.

dc-bus var compensator is the most widely known [17]. In [18], an external excitation circuit for a SEIG was proposed. The effective external capacitive reactance can be varied through the switching of inductances. The switching is performed using electronic power switches, the action being commanded by the voltage controller. Since each leg of the delta connected inductor can be controlled independently, this configuration can easily handle unbalanced generator loads.

Let us consider that the machine has an initial residual flux (or some means are provided to inject an initial current into the stator windings), and the rotor is propelled by some external mechanical power source, such as an fuel engine, hydraulic turbine, etc. If external capacitors of adequate values are connected to the stator windings, self excitation occurs. The magnitude of the generated voltage will depend among other things on the capacitance value, the load current, and the load power factor. Considering steady state operation it is possible to observe three regions clearly differentiated: i) a *stable zone*, corresponding to operation in the saturated region of the magnetic core; ii) an *unstable zone*, corresponding to operation on the linear region of the magnetic core; and iii) a region of *no-generation*. In the first case, the linear I-V curve of the excitation capacitors intersect the core magnetizing curve at a well defined point. In the second case, the intersection is not well defined, for it occurs at an infinite number of points. In the third case, the only intersection occurs at the origin as is shown in Fig. 1.

Let us assume that the machine is actually operating at point 1 in Fig. 1. If a capacitor of value C_2 is connected, the new generated voltage will be determined by the machine characteristic curve, and will evolve from point 1 to point 2 with a definite time constant. Conversely, if the capacitor is reduced from a value C_1 at point 1 to a value C_0 , smaller than C_1 , the magnetizing current will not be compensated by

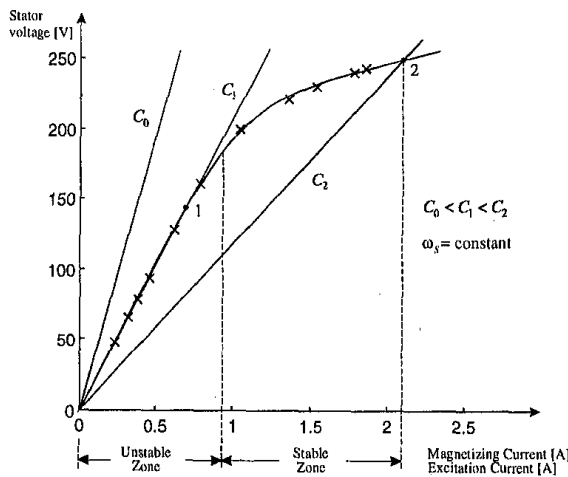


Fig. 1. Magnetizing characteristic of a SEIG (experimental points are marked with \times).

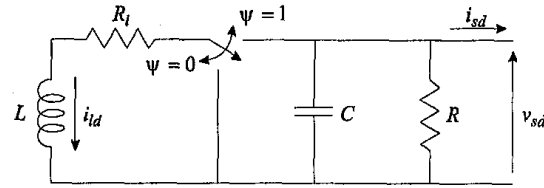


Fig. 2. d -axis representation of the external excitation circuit (q -axis representation is identical).

an identical but leading current component. In this case, the machine will first try to save the situation by dropping some of its magnetizing current in order to reach another stable operating point along its magnetizing curve. This results in a lower air gap voltage and a consequently lower flux; the slip will increase and finally the machine will stop generating (intersection at zero in Fig. 1). Fortunately, the time constants involved in either situation (voltage increase or decrease) are lower than the generation period, this fact allows corrective commutation actions to be taken to keep the average leading current around its required value. First order information of the constants can be obtained from a linearized analysis around the operating point.

In principle, it should be possible to stay in the neighborhood of point 1 by means of some kind of clever capacitor switching (between values C_0 and C_2) such that in average the correct magnetizing current is provided. However, direct capacitor switching is not convenient because excessive current surges occur at the switching instants. An alternative configuration is shown in Fig. 2 [18]. Here a equivalent representation in a $d-q$ stationary reference frame was used for a symmetrical, balanced, three-phase system [19]. As before, C is the excitation capacitance (the value of which exceeds C_1); L is an external inductance, with internal resistance R_l ; R is the load resistance; i_{sd} and i_{sl} are the stator and inductance currents respectively; and v_{sd} is the stator voltage; the subscript d denotes the d -phase of the (d,q) reference frame. When the inductance L is connected in parallel to the capacitor C (control action $\psi = 1$) the equivalent capacitive reactance X_{LC} is greater than the original capacitor reactance. To increase momentarily the equivalent capacitance, the inductance is disconnected from the circuit (control action $\psi = 0$); the inductive current finds its path along the circuit formed by R_l and L .

In order to guarantee the generation under different load conditions, it is necessary to observe the following steps: i) Find the feasible range of load impedances $Z_{\min} < Z < Z_{\max}$; ii) Determine analytically the minimum capacitance value C_{\min} that guarantees the self excitation condition, and choose $C > C_{\min}$; and iii) Calculate L , such that L in parallel with C behaves as an equivalent capacitor lower

than C_{\min} . For a given generator, $\|Z_{\min}\|$ will be roughly determined by the maximum allowable output power. C_{\min} can be determined from the generator electrical parameters, following methods such as those detailed in [2, 3] and [20] among others.

III. CONTROL STRATEGY

The control strategy proposed here has the objective of controlling simultaneously the output voltage and the frequency of a SEIG, operating in the linear region of the core magnetizing curve. Techniques based on variable structure control are used. The main advantages of this control theory are obtained incorporating sliding modes [9, 10]. The basic idea of sliding mode controllers is to force the dynamic system trajectory to move on a switching surface appropriately designed in the system state space. Sliding mode occurs when the states are forced to remain on the switching surface by means of appropriate switching actions.

A. Salient Aspects of the Voltage Control

In order to perform the following analysis, a dynamic model of the induction generator (IG) [19] plus the external excitation circuit is used. The electromagnetic dynamic model of a three-phase squirrel-cage induction machine can be expressed in the $d-q$ stationary reference frame. The stator voltage can be represented as a vector

$$\mathbf{v}_s(t) = v_{sd}(t) + jv_{sq}(t),$$

the magnitude of which is:

$$V_s(t) = \|\mathbf{v}_s(t)\| = \sqrt{(v_{sd}(t))^2 + (v_{sq}(t))^2};$$

v_{sd} and v_{sq} are the d and q voltage components respectively. The control objective is to keep $V_s(t) = \|\mathbf{v}_s(t)\|$ as close as possible to a reference value $V_{sref} > 0$, for all load conditions. In order to satisfy the control objective we propose here the use of variable structure control strategies. It would be natural to define the following switching surface:

$$S_v(t) = V_s(t) - V_{sref} = 0. \quad (1)$$

If we are able to sustain the system in sliding mode, that is $S_v(t) = 0$, the control objective will be satisfied, i.e. $V_s(t) = V_{sref}$. However, (1) is not convenient for control purposes. The reason is that $V_s(t)$ contains high frequency components which produce very fast switching on the proposed surface.

The voltage equation for the stator windings may be expressed by

$$\mathbf{v}_s(t) = R_s \mathbf{i}_s(t) + \frac{d}{dt} \lambda_s(t), \quad (2)$$

where \mathbf{i}_s and λ_s denote stator current and stator flux vector respectively, and R_s is the per-phase stator winding resistance. From (2) we obtain

$$\lambda_s(t) = \int (\mathbf{v}_s(t) - R_s \mathbf{i}_s(t)) dt.$$

λ_s has lower energy content at high frequencies than \mathbf{v}_s . Let us define a new switching surface as follows:

$$S_{\lambda_s}(t) = \|\lambda_s(t)\| - \lambda_{sref}(t) = 0, \quad (3)$$

where λ_{sref} is an appropriate stator flux-norm reference value, such that when the system slides on (3) the control objective $V_s(t) = V_{sref}$ is satisfied. Since the stator flux vector λ_s is an unmeasured variable, it will be replaced by its observed value, $\hat{\lambda}_s$. In [21] a Variable Structure Rotor Flux Observer for a SEIG is proposed; stator flux can be directly obtained from the rotor flux [19].

When the generator load changes, it is necessary to modify the magnetizing flux, and consequently the stator flux, in order to keep $V_s(t)$ at the reference value. λ_{sref} cannot be constant because, in that case, sliding condition (3) would imply that $V_s(t) = V_{sref}$ is not necessarily true. Keeping $V_s(t) = V_{sref}$ involves that λ_{sref} must be adapted in some way. Let us define

$$\lambda_{sref}(t) = \lambda_{srefnom} + k_i \int (V_{sref} - V_s(t)) dt,$$

where $\lambda_{srefnom}$ is the stator flux reference value for any particular IG operating condition, and k_i is a constant. $S_{\lambda_s} > 0$ implies $\|\hat{\lambda}_s(t)\| > \lambda_{sref}(t)$, and in stationary conditions it implies $V_s(t) > V_{sref}$. In order for $V_s(t)$ to decrease, it is imperative that the excitation current supplied by the external circuit decrease. This is obtained connecting the inductances in parallel to the external capacitors ($\psi = 1$) in such a way that $X_{LC} > X_{Cmin}$. On the contrary, $S_{\lambda_s} < 0$ indicates $\|\hat{\lambda}_s(t)\| < \lambda_{sref}(t)$, and in stationary state it implies $V_s(t) < V_{sref}$. In this case, the external circuit should provide the extra excitation necessary to increase the magnetizing current. This is obtained disconnecting the inductances from the circuit ($\psi = 0$). Consequently, a discontinuous control action is devised:

$$\psi = \begin{cases} 0 & \text{if } S_{\lambda_s} < -\varepsilon, \\ 1 & \text{if } S_{\lambda_s} > \varepsilon, \\ \text{it keeps its} & \text{if } |S_{\lambda_s}| \leq \varepsilon. \\ \text{last value} & \end{cases} \quad (4)$$

A tolerance band of width 2ε is introduced to reduce the switching frequency of the electronic elements. Within this band no changes in the control action ψ are performed.

The discontinuous control action (4) forces the dynamic system to commute between two structures clearly differentiated: i) *stable mode* ($\psi=1$), in which the output voltage V_s tends to decrease; and ii) *unstable mode* ($\psi=0$), in which the output voltage tends to increase.

Fig. 3 shows the evolution of the stator voltage vector norm, V_s , for different switching instants. In this simulation, the generator excitation was maintained ($\psi=0$) until the voltage magnitude V_s was near to 100V. From that moment on, the inductances were connected at slightly different times t_{on} (and consequently different phase angles between \mathbf{v}_s and \mathbf{i}_l). The initial inductance current was $\|\mathbf{i}_l\| = 0.6$ A and the load was a 100Ω resistance. The curves correspond to the initial phase differences shown in Table 1.

From Fig. 3, it can be observed a non monotonous behavior of $V_s(t)$ following the connection of the external inductances. If the instantaneous angle between \mathbf{i}_l and \mathbf{v}_s is not properly chosen, the transient can even exhibit inverse response. If the objective is to reduce immediately the magnitude of V_s at the connection instant, it is necessary that the initial phase value be in the interval $-90^\circ < \text{phase}(\mathbf{i}_l, \mathbf{v}_s) < 90^\circ$, otherwise, there will be an initial inverse response behavior.

At steady state, when the stator voltage is controlled in the neighborhood of the reference value, the inductance current vector lags 90° with respect to \mathbf{v}_s . Fig. 4 shows a reference frame fixed to \mathbf{v}_s (that is, it rotates following \mathbf{v}_s). If the inductances are connected when \mathbf{i}_l lags more than 90° , then \mathbf{i}_l moves forward to satisfy $\text{phase}(\mathbf{i}_l, \mathbf{v}_s) \equiv -90^\circ$, and keeps rotating, following \mathbf{v}_s . When the inductances are disconnected, \mathbf{i}_l is no more joined to the system (i.e., \mathbf{i}_l

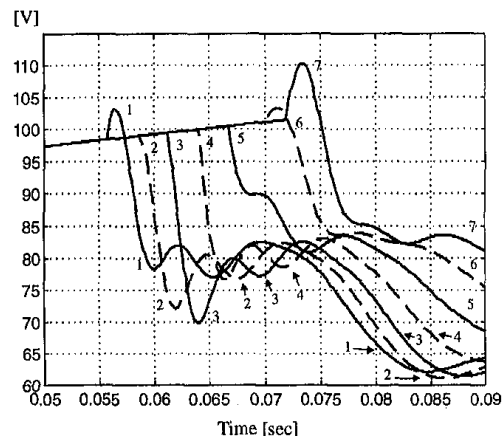


Fig. 3. Evolution of $V_s(t)$ for different inductance connection instants (see Table 1).

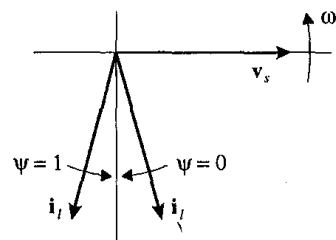


Fig. 4. Phase diagram of \mathbf{v}_s and \mathbf{i}_l .

stops rotating), and then $\text{phase}(\mathbf{i}_l, \mathbf{v}_s)$ increases at the rate $\omega_s t$, where ω_s is the angular frequency of \mathbf{v}_s . What happens while the controller is actuating, is that before the phase lag becomes too large, $\psi=1$ is issued and \mathbf{i}_l rotates at an average angular frequency ω_s following \mathbf{v}_s .

It is highly desirable that the actions taken to control V_s do not affect substantially the instantaneous generation angular frequency $\omega_s(t)$. Fig. 5 shows the behavior of $\omega_s(t)$ as it results from the different connection instants. Larger variations occur when $0^\circ < \text{phase}(\mathbf{i}_l, \mathbf{v}_s) < 90^\circ$. The least variation occurs when $\text{phase}(\mathbf{i}_l, \mathbf{v}_s)$ approaches -90° .

Consequently, the information provided by the surface (3) and the control action (4) do not suffice to produce a smooth control of the voltage magnitude. In the light of the preceding results, it seems reasonable that in order to produce $\psi=1$, in addition to the condition $S_{\lambda_s} > \varepsilon$, be required that the phase lag of \mathbf{i}_l be slightly smaller than 90° . Since it is possible to calculate the maximum rate of increase of V_s , waiting for the phase to be within the prescribed bounds implies no more than an accountable ripple in the voltage magnitude.

Table 1: PHASE ANGLE BETWEEN \mathbf{i}_l AND \mathbf{v}_s AT t_{on} .

Curve N°	Phase ($\mathbf{i}_l, \mathbf{v}_s$)
1	135°
2	90°
3	45°
4	0°
5	-45°
6	-90°
7	-135°

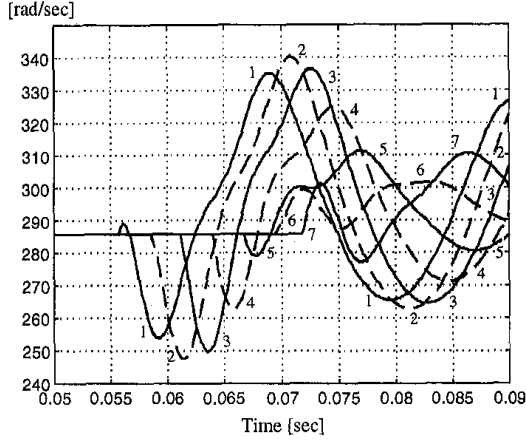


Fig. 5. Evolution of $\omega_s(t)$ for different inductance connection instants (see Table 1).

B. Frequency Control

Once the generator reaches its steady-state operating condition, the generation angular frequency $\omega_s(t)$ will remain constant. This stationary value is given by:

$$\omega_s(t) = n_p \omega_r(t) - \omega_{sl}(t), \quad (5)$$

where n_p is the number of pole pairs, ω_r is the mechanical rotor speed and ω_{sl} is the slip angular frequency. The generation frequency can be modified around its steady value simply by varying appropriately the rotor speed. Consequently, frequency control reduces to modifying adequately rotor speed by means of the externally applied torque.

It becomes imperative that speed control be robust and insensitive to parameter variations. There are several alternatives to fulfill the above requirements [13, 14]. In this paper, we present a strategy based on VSC. A control action is devised that forces the system to evolve on an adequate switching surface even in the presence of disturbances. Once the system reaches the surface and slides on it, the angular frequency error will converge to zero with first order behavior.

The dynamics of the rotor can be modeled as:

$$\dot{\omega}_r(t) = \frac{1}{J} \{-B\omega_r(t) - T_{elec}(t) + T_{mec}(t)\},$$

where J is the rotor inertia, B is the viscous friction coefficient, T_{elec} is the electromagnetic torque and T_{mec} is the external mechanical torque applied to the machine.

For convenience, let us define the angular frequency error:

$$x_1(t) = \omega_{sref} - \omega_s(t),$$

where ω_{sref} is the reference value, that we will assume constant. Consequently,

$$\begin{aligned} \dot{x}_1(t) &= -\dot{\omega}_s(t) = -n_p \dot{\omega}_r(t) + \dot{\omega}_{sl}(t) \\ &= an_p \omega_r(t) - b\{T_{mec}(t) - T_{elec}(t)\} + \dot{\omega}_{sl}, \end{aligned} \quad (6)$$

where $a = B/J$, $b = n_p/J$.

Furthermore, we define:

$$x_2(t) = -n_p \dot{\omega}_r(t) = \dot{x}_1(t) - \dot{\omega}_{sl}(t). \quad (7)$$

Taking the time derivative of (7), we get:

$$\dot{x}_2(t) = an_p \dot{\omega}_r(t) - bU, \quad (8)$$

where $U = \frac{d}{dt}\{T_{mec}(t) - T_{elec}(t)\}$.

The system represented by (6) and (8) becomes to

$$\begin{bmatrix} \dot{x}_1 \\ \dot{x}_2 \end{bmatrix} = \begin{bmatrix} 0 & 1 \\ 0 & -a \end{bmatrix} \begin{bmatrix} x_1 \\ x_2 \end{bmatrix} + \begin{bmatrix} 0 \\ -b \end{bmatrix} U + \begin{bmatrix} 1 \\ 0 \end{bmatrix} \dot{\omega}_{sl}. \quad (9)$$

It remains now to define the control action U . In most applications, it is convenient that the dynamic response of the error x_1 be fast and without overshoots. This can be obtained using a switching surface defined by:

$$S_{\omega_s 1}(t) = cx_1(t) + x_2(t) = 0. \quad (10)$$

The larger the value of c in equation (10), the faster the speed of response. However, if the initial velocity error is too large, the system will reach the switching surface $S_{\omega_s 1}$ with an excessive acceleration. Then, in addition to the surface $S_{\omega_s 1}$ we can introduce additional surfaces $S_{\omega_s 2}$ and $S_{\omega_s 3}$ to limit the maximum attainable acceleration and to reduce the requirements of the external mechanical torque. The additional surfaces are described by:

$$S_{\omega_s 2}(t) = -|x_{2max}| + x_2(t) = 0,$$

$$S_{\omega_s 3}(t) = +|x_{2max}| + x_2(t) = 0.$$

It can be observed that on the surfaces $S_{\omega_s 2}$ and $S_{\omega_s 3}$ the system evolves with constant acceleration and consequently this surfaces are responsible to limit the maximum acceleration of the rotor, while the surface $S_{\omega_s 1}$ drives the state (x_1, x_2) towards the origin of the phase plane. On $S_{\omega_s 2}$ and $S_{\omega_s 3}$, $x_1(t)$ evolves describing ramps, while on $S_{\omega_s 1}$, $x_1(t)$ shows a first order response with time constant $1/c$. The switching surfaces $S_{\omega_s 1}$, $S_{\omega_s 2}$ and $S_{\omega_s 3}$ do not depend on the system parameters (a, b) . Then, using VSC it is possible to force the frequency error to follow predefined

dynamics, independent of variations in the parameters of the plant.

Whenever a frequency errors occurs, the state trajectory in the phase plane will be directed towards the switching surface. Once the state reaches the surface, the system will slide on it towards the origin of the phase plane, provided that an adequate control action is taken. The following control law provides a fast reaching and a very low chattering at steady state

$$U = \varphi_1 x_1 + \varphi_2 x_2 + K \operatorname{sgn}(S_{\omega_s}), \quad (11)$$

where

$$\varphi_1 = \begin{cases} \alpha_1 & \text{if } S_{\omega_s} x_1 > 0, \\ \beta_1 & \text{if } S_{\omega_s} x_1 < 0, \end{cases} \quad \varphi_2 = \begin{cases} \alpha_2 & \text{if } S_{\omega_s} x_2 > 0, \\ \beta_2 & \text{if } S_{\omega_s} x_2 < 0, \end{cases}$$

and $\operatorname{sgn}(\cdot)$ is the sign function defined as

$$\operatorname{sgn}(S_{\omega_s}) = \begin{cases} +1 & \text{if } S_{\omega_s} > 0, \\ -1 & \text{if } S_{\omega_s} < 0, \end{cases}$$

K is a scalar to be defined, and S_{ω_s} represents any of the surfaces $S_{\omega_{s1}}$, $S_{\omega_{s2}}$, or $S_{\omega_{s3}}$. The first term in (11) (the proportional term) is the standard control law used in VSC [22], whereas the second and third terms are introduced to improve the rejection to disturbances and to obtain a faster reaching mode.

The controller gains (φ_1 , φ_2 , and K) can be evaluated based on the existence conditions for sliding mode, [22], given by:

$$\lim_{S_{\omega_s} \rightarrow 0} S_{\omega_s} \dot{S}_{\omega_s} < 0.$$

When applied to the surface $S_{\omega_{s1}}$, equations (9), (10) and (11) give:

$$S_{\omega_s} \dot{S}_{\omega_s} = (c - a - b\varphi_2)x_2 S_{\omega_s} - b\varphi_1 x_1 S_{\omega_s} + \left\{ c\dot{\omega}_{sl} - bK \operatorname{sgn}(S_{\omega_s}) \right\} S_{\omega_s}.$$

Considering the definition of φ_1 and φ_2 given by equation (11), the existence condition can be guaranteed if:

$$\beta_1 < 0 < \alpha_1; \quad \beta_2 < \left| \frac{c-a}{b} \right| < \alpha_2; \quad \text{and } K > \frac{\delta}{b}; \quad (12)$$

where $\delta \geq |c\dot{\omega}_{sl\max}|$. It can be observed from (12) that the maximum value for the slope c of $S_{\omega_{s1}}$ is limited by the

gains α_2 and β_2 . Note that is not necessary to know $\dot{\omega}_{sl}$, only an upper bound over its value is required.

For the constant acceleration surfaces $S_{\omega_{s2}}$ and $S_{\omega_{s3}}$, bounds on the coefficients φ_1 and φ_2 are obtained making zero the slope term in $S_{\omega_{s1}}$ that is, $c=0$ in equation (10). Hence, the bounds are given by:

$$\beta_1 < 0 < \alpha_1; \quad \beta_2 < \left| -\frac{a}{b} \right| < \alpha_2; \quad \text{and } K > 0.$$

It is worth to note that the controller design does not require a precise knowledge of the system parameters.

The mechanical torque applied to the generator rotor will be:

$$T_{mec} = \int \left\{ \varphi_1 x_1 + \varphi_2 x_2 + K \operatorname{sgn}(S_{\omega_s}) \right\} dt + T_{elec}. \quad (13)$$

The integral in (13) will have the effect of filtering the high frequency switching produced by the relay-like term $K \operatorname{sgn}(S_{\omega_s})$.

IV. SIMULATION RESULTS

The parameters used in the simulation are: $R_s = 8.74\Omega$; $R_r = 8.15\Omega$; $L_s = L_r = 692\text{mHy}$; $M = 656\text{mHy}$; $R_l = 1\Omega$; $L = 422\text{mHy}$; $C = 34\mu\text{F}$; $n_p = 2$;

$J = 0.005\text{Nmseg}^2/\text{rad}$; and $B = 0.0038\text{Nmseg}/\text{rad}$. The nominal characteristics of the machine when acting as a motor are: power: 0.75kW ; voltage: $220/380\text{V}$; current: $3.7/2.1\text{A}$; and frequency: 50Hz . The reference values for voltage and frequency control were fixed at: $V_{sref} = 100\text{V}$, and $\omega_{sref} = 314.16\text{rad/sec} = 2\pi 50\text{rad/Hz}$. The voltage control parameters are: $k_i = 0.0982$; and $\varepsilon = 5e^{-4}\text{Wb}$. The frequency control parameters are: $\alpha_1 = 0.5\text{Nm/rad}$; $\beta_1 = -0.5\text{Nm/rad}$; $\alpha_2 = 0.25\text{Nmsec/rad}$; $\beta_2 = -0.25\text{Nmrad/sec}$; $K = 5\text{Nm/sec}$; and $c = 8\text{sec}^{-1}$. Experimental points of the machine magnetizing curve are shown in Fig. 1.

The SEIG simulation was performed considering an initial stator current of $i_{sd} = i_{sq} = 1\text{A}$, a rotor speed of $\omega_r = 314\text{rad/sec}$, and a electric load of $R = 800\Omega$.

The simulation consists of two stages. Firstly, from $t = 0$ sec the electrical excitation is allowed ($\psi = 0$); the stator voltage grows from $V_s = 0V$ to $V_s = 100V$. When V_s reaches $100V$, the voltage control action keeps it close to the reference value, such as shown in Fig. 6. At $t = 0.4$ sec, the electric load is changed from $R = 800\Omega$ to $R = 100\Omega$. The voltage drops momentarily and quickly recovers its value. Finally, at $t = 1$ sec the electric load is changed from $R = 100\Omega$ to $R = 200\Omega$.

The generation angular frequency and the rotor angular speed are shown in Fig. 7. While the stator voltage is controlled at its reference value before $t = 0.4$ sec, the generation angular frequency is kept at its reference value of $\omega_{sref} = 314.16 \text{ rad/sec}$. When the electric load is changed at $t = 0.4$ sec, the slip frequency increases. As the rotor speed cannot be varied instantaneously, the generation frequency drops. The recovery (after $t = 0.4$ sec) is dominated by the rotor mechanical time constant. To bring the angular frequency ω_s back to its reference value, it is necessary to increase the rotor speed through the external mechanical torque. The angular frequency error tends to zero with a time constant given by $1/c$.

The external mechanical torque is shown in Fig. 8. When the angular frequency error increases at $t = 0.4$ sec, the mechanical torque tries to reduce the error increasing its value, i.e. accelerating the rotor.

V. CONCLUSIONS

In this paper the self excitation process of a SEIG was analyzed. An external excitation circuit was used. Control strategies for both voltage and frequency were presented, based on Variable Structure Control theory. A detailed analysis was performed, showing some salient aspects

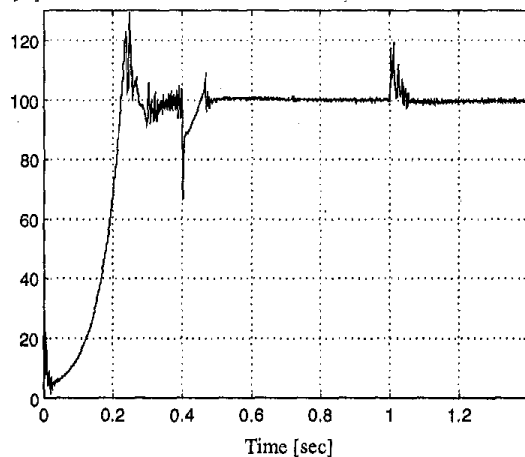


Fig. 6. Norm of stator voltage vector, $V_s(t) = \|v_s(t)\|$; $V_{sref} = 100 \text{ V}$.

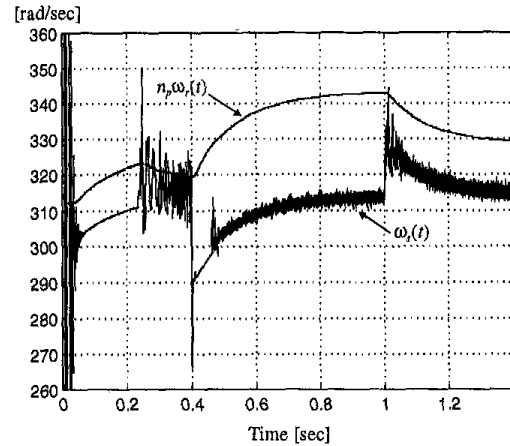


Fig. 7. Generation angular frequency, $\omega_s(t) [\text{rad/sec}]$, and rotor angular speed, $n_p \omega_r(t) [\text{rad/sec}]$; $\omega_{sref} = 314.16 \text{ rad/sec}$.

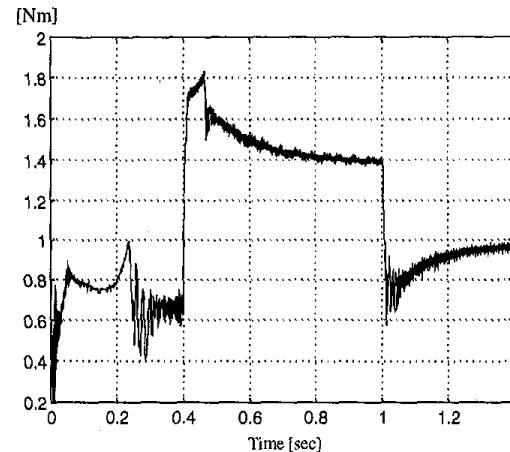


Fig. 8. External mechanical torque, $T_{mec}(t) [\text{Nm}]$.

related to the connection of the external excitation circuit on the control performance.

Computer simulation were used to show the dynamic performance of the proposed scheme.

The subject of ongoing studies is to make experimental validation of the present results.

VI. REFERENCES

- [1] A. Langdorf, *Theory of Alternating-Current Machinery*. McGraw-Hill, Second Edition, 1955.
- [2] N. Malik, and S., Haque, "Steady State Analysis and Performance of an Isolated Self-Excited Induction Generator." *IEEE Trans. on Energy Conversion*, vol. EC-1, no. 3, Sept. 1986, pp. 134-140.
- [3] T. Chan, "Capacitance Requirements of Self-Excited Induction Generators." *IEEE Trans. on Energy Conversion*, vol. 8, no. 2, June 1993, pp. 304-311.
- [4] L. Shridhar, B. Singh, and C. Jha, "Transient Performance of the Self Regulated Short Shunt Self Excited Induction Generator." *IEEE Trans. on Energy Conversion*, vol. 10, no. 2, June 1995, pp. 261-267.

- [5] O. Ojo, "Performance of Self-Excited Single-Phase Induction Generators with Shunt, Short-Shunt and Long-Shunt Excitation Connections." *IEEE Trans. on Energy Conversion*, vol. 11, no. 3, Sept. 1996, pp. 477-482.
- [6] L. Yegna, S. Narayanan, and V. Johnny, "Contributions to the Steady State Analysis of Wind-Turbine Driver Self-Excited Induction Generators." *IEEE Trans. on Energy Conversion*, vol. EC-1, no. 1, March 1986, pp. 169-176.
- [7] A. Beluco, R. Brito, R. Homrich, F. Livi, and I. Motchalov, "Controle de Tensão e Freqüência em Geradores Assíncronos Independentes." 7° *Congreso Latinoamericano de Control Automático, XV Simposio Nacional de Control Automático*, Sept. 1996, pp. 133-139, Buenos Aires, Argentina.
- [8] T. Chan, "Self-Excited Induction Generators Driven by Regulated and Unregulated Turbines." *IEEE Trans. on Energy Conversion*, vol. 11, no. 2, June 1996, pp. 338-343.
- [9] V. Utkin, "Variable Structure Systems with Sliding Modes." *IEEE Trans. on Automatic Control*, vol. AC-22, no. 2, April 1977, pp. 212-222.
- [10] J. Hung, W. Gao, and J. Hung, "Variable Structure Control: A Survey." *IEEE Trans. on Industrial Electronics*, vol. 40, no. 1, February 1993, pp. 2-22.
- [11] A. Sabanovic, and D. Izosimov, "Application of Sliding Modes to Induction Motor Control." *IEEE Trans. on Industry Applications*, vol. IA-17, no. 1, January 1981, pp. 41-49.
- [12] V. Utkin, "Sliding Mode Control Design Principles and Applications to Electric Drives." *IEEE Trans. on Industrial Electronics*, vol. 40, no. 1, February 1993, pp. 23-36.
- [13] E. Ho, and P. Sen, "Control Dynamics of Speed Drive Systems Using Sliding Mode Controllers with Integral Compensation." *IEEE Trans. on Industry Applications*, vol. 27, no. 5, Sept. 1991, pp. 883-892.
- [14] K. Shyu, and H. Shieh, "A New Switching Surface Sliding-Mode Speed Control for Induction Motor Drive Systems." *IEEE Trans. on Power Electronics*, vol. 11, no. 4, July 1996, pp. 660-667.
- [15] M. Brennen, and A. Abbondanti, "Static Exciters for Induction Generators." *IEEE Trans. on Industry Applications*, vol. IA-13, no. 5, Sept. 1977, pp. 422-428.
- [16] F. Peng, and J. Lai, "Dynamic Performance and Control of a Static Var Generator Using Cascade Multilevel Inverters." *IEEE Trans. on Industry Applications*, vol. 33, no. 3, May 1997, pp. 748-755.
- [17] L. Moran, P. Ziogas, and G. Joos, "Analysis and Design of a Three-Phase Current Source Solid-State Var Compensator." *IEEE Trans. on Industry Applications*, vol. 25, no. 2, March 1989, pp. 356-365.
- [18] E. Suárez, G. Bortolotto, and M. Colantonio, "Control por Estructura Variable de Tensión y Frecuencia de un Generador de Inducción Autoexcitado." 7° *Congreso Latinoamericano de Control Automático, XV Simposio Nacional de Control Automático*, Sept. 1996, pp. 211-216, Buenos Aires, Argentina.
- [19] P. Krause, O. Wasynczuk, and S. Sudhoff, *Analysis of Electric Machinery*. IEEE Press, 1995.
- [20] O. Ojo, "Minimum Airgap Flux Linkage Requirement for Self-Excitation in Stand-Alone Induction Generators." *IEEE Trans. on Energy Conversion*, vol. 10, no. 3, Sept. 1995, pp. 484-492.
- [21] E. Suárez, G. Bortolotto, and C. Muravchik, "Variable Structure Rotor Flux Observer for a Self Excited Induction Generator." *Latin American Applied Research*, vol. 27, no. 3, Sept. 1997, pp. 161-167.
- [22] V. Utkin, *Sliding Modes in Control and Optimization*. Springer-Verlag, 1992.

VII. BIOGRAPHIES

Eduardo Suárez was born in Río Cuarto, Argentina, on September 10, 1967. He received the B.Sc. degree in electrical engineering from Universidad Nacional de Río Cuarto, Argentina, in 1993. He is currently working toward the M.Sc. degree in Control Systems at Universidad Nacional del Sur, Argentina. His research interests are in the areas of control of electric machines and control applications.

Gustavo Bortolotto was born in Argentina, on October 28, 1951. He received his electrical engineering degree from Universidad Nacional del Sur (UNS), Argentina in 1976 and his Ph.D. degree from The Technical University of Denmark in 1985. He is currently Associate Professor at the Department of Electrical Engineering, UNS, Argentina. His research interests include electronics, multivariable control systems and digital control for electric machinery.